Journal of the European Ceramic Society 18 (1998) 1695–1705

PII: S0955-2219(98)00090-9
0955-2219/98/$—see front matter

Compositional Fluctuations and Properties of Fine-Grained Acceptor-Doped PZT Ceramics

J. F. Fernández,[a]* C. Moure,[a] M. Villegas,[a] P. Durán,[a] M. Kosec[b] and G. Drazic[b]

[a]Electroceramics Department, Instituto de Cerámica y Vidrio, CSIC, 28500 Arganda del Rey, Madrid, Spain
[b]Jozef Stefan Institute, 1001 Ljubljana, Slovenija

(Received 10 September 1997; accepted 4 March 1998)

Abstract

Fine-grained acceptor-doped lead zirconate titanate (PZT) ceramics were sintered in a wide range of temperatures and times. The differences in dielectric and piezoelectric properties were relevant and quite independent of grain size. The incorporation of acceptor dopant into the solid solution of PZT was responsible for the change of properties, the evolution of secondary phases and the weight loss behaviour. The PbO rich phase located between grains displaced from the PbO–PZT system to PbO–PZ system when iron cations entered the PZT lattice. At this time, precipitated monoclinic grains of zirconia among with tetragonal perovskite grains revealed the compositional fluctuations. After the iron cations entered into solid solution the liquid formed dissolved new PZT grains again and displaced to PbO–PZT system with increasing of weight loss. Decomposition experiments revealed also the nature and the evolution of the second phases that are in accordance with TEM observations. © *1998 Elsevier Science Limited. All rights reserved*

1 Introduction

Lead zirconate titanate (PZT) ceramics are widely used as a piezoelectric in different applications. The ceramic materials possess several advantages over single crystals: they are easy to produce and machine in different shapes and with tailored properties because of chemical modifications introduced by dopants. The highest piezoelectric coupling coefficients have been found near the morphotropic phase boundary[1] (MPB) where coexistence of the tetragonal, Ti-rich phase, and rhombohedral, Zr-rich phase, appears. The MPB has believed to be a sharp transition, but in practice the MPB has a finite range of compositions over which the tetragonal and rhombohedral phases coexist. The width of the MPB has been investigated by many authors and found to be related to the heterogeneous distribution of Zr^{4+} and Ti^{4+} cations on the B site of the perovskite lattice.[2,3] The compositional fluctuations were smaller for coprecipitated or sol–gel produced ceramics.[4,5] Even the monophasic perovskite ceramics of the MPB composition, or near the MPB, became two-phase materials with the lapse of time after poling.[5] The effect of compositional fluctuations on the properties of PZT has been also reported.[4,6,7] The compositional fluctuations in PZT samples decreased with increasing calcination temperatures and times in the range of 760–860°C and 1–5 h.[6] A further increase in the calcination temperature was not very effective because of the lack of stoichiometry caused by PbO evaporation. The extent of compositional fluctuations was also very sensitive to the sintering conditions and the atmosphere control used during sintering. Very high sintering temperatures, 1350°C, gave free ZrO_2 precipitates because of the PbO loss by evaporation according with the following reaction proposed by Saha and Agrawal:[6]

$$Pb(Zr_xTi_{1-x})O_3 \rightarrow Pb_{(1-\Delta)}(Zr_{x-\delta}Ti_{1-x})O_{3-\Delta-2\delta} + \Delta PbO + \delta ZrO_2 \quad (1)$$

There is also a significant increase in the c/a ratio of the tetragonal phase mainly by shrinkage of a parameter. Such a phenomenon has been reported to be dependent on the distance from the surface for samples fired in low lead vapour pressures.[7] The width of the zone where ZrO_2 precipitated appeared was about 150 μm for samples sintered at 1300°C. Recently, the displacement of PZT with a

*To whom correspondence should be addressed. Fax: 0034 1 870 0550; e-mail: jfernandez@icv.csic.es

morphotropic composition toward the $PbTiO_3$-rich region for temperatures above 1100°C has been reported,[8] although zirconia phases could not be confirmed by XRD analysis of the ceramic matrix. Similar results were attained for thick porous films but with the appearance of PbO crystalline precipitates as a second phase on PZT skeleton.[8] Even though the PbO activity is the main reason for the described phenomenon, up to now the decomposition mechanism is not well understood. So, several questions need to be answered in order to further control of decomposition effects in PZT ceramics. The practical aspect of such an understanding is its relevance to the lack of reproducibility from batch to batch in the industrial manufacturing. In this paper, an approach to the origin of such a decomposition mechanisms, its relationship with compositional fluctuations, and its influence on the final properties is attempted.

2 Experimental Procedure

Lead zirconate titanate ceramics near the MPB composition were prepared following a previously described procedure of the mixed oxide calcination route.[9] The selected composition was:

$$Pb_{1.000}(Zr_{0.530}Ti_{0.458}Fe_{0.010}Nb_{0.002})O_{3-\delta} \quad (2)$$

No excess of lead oxide was used. Nb^{5+} formed part of the TiO_2 anatase raw materials and was used as a controlled impurity. The 0·5 mol% of $FeO_{1.5}$ per mol of PZT (0·5 atoms% of Fe^{3+} or 0·8 wt% of Fe_2O_3) addition was chosen to be on the solid solution limit in order to avoid an excess of acceptor-cations. For that reason, it was assumed that Nb^{5+} cations were compensated by Fe^{3+} ones.

Fine grained high purity raw materials were homogenised by ball milling in isopropyl alcohol media for 3 h, dried, sieved, and calcined at 800°C for 4 h. No weight loss was detected at that step. After the calcining process these powders were milled in a two step milling process: 3 h ball milled and thereafter 3 h attrition milled. Both processes were performed with stabilised zirconia balls in isopropyl alcohol media. Powders were pressed isostatically at 200 MPa and sintered between 1070 and 1190°C for 2 h, and at 1150°C for 1 to 8 h. $PbZrO_3$ + 5 wt% ZrO_2 was used as an atmosphere buffer in sealed alumina crucibles.[10] Weight loss was controlled by weighting samples before and after sintering. Bulk densities of sintered samples were determined by the Archimedes method. Phase identification was attained by XRD (Siemens D5000) using CuK_α radiation. 50 kV, 30 mA and a scan rate of 0·5° min^{-1} were used as standard conditions. 2θ angles from 43 to 46° were explored at 0·1° min^{-1} in order to determine the tetragonal and rhombohedral phase content of sintered samples. For such a purpose, sintered samples were polished and annealed at 400°C in order to reduce preferential orientations due to grinding.[11] For determination of rhombohedral/tetragonal phase content pseudo-Voigt functions were used, the reliability of the deconvolution was $< 10\%$ and integrated peaks were used to determine the rhombohedral/tetragonal ratio.

Microstructural development of the samples were examined by using scanning electron microscopy (SEM, Zeiss D950), and transmission electron microscopy (TEM, Jeol 2000FX) operating at 200 kV, with energy dispersive spectroscopy (EDS, EM Link AN 10000) having a probe size resolution of approximately 15 nm. Several spectra were collected for each composition and little variation was seen between them. Average grain size of ceramic was determined for polished and chemically etched surfaces by the linear intercept technique.

Disks of 12 mm in diameter and 1 mm thickness, obtained by cutting with a diamond saw and then polished, were electroded with silver paste. The electrodes were sintered at 800°C during 10 min. The dielectric measurements were performed using a 4192A HP Impedance Analyzer at room temperature at 1 kHz. The ceramics were poled at 120°C for 15 min under a field of 40 kV cm^{-1} in a silicone bath. Piezoelectric parameters were measured 24 h after poling following IRE standard.[12]

The decomposition experiments were performed on polished surface of samples sintered at 1150°C for 2 and 8 h following the crystalline evolution by XRD.

3 Results

3.1 Microstructure development

The average particle size of synthesized powders was $d_{50} = 0{\cdot}85\ \mu m$. Both the fine grained raw materials used and the effectiveness of the double milling procedure allowed the production of very reactive powders from conventional solid state reaction route. Such a powder densified up to $> 97\%$ of the theoretical density, 8·00 g cm^{-3}, at lower temperatures than conventional PZT ceramics (Fig. 1). The ceramics sintered to nearly complete densification in a wide range of temperatures and times. On the other hand, the weight loss increased for samples sintered at temperatures higher than 1150°C, and also increased gradually with the sintering time at 1150°C.

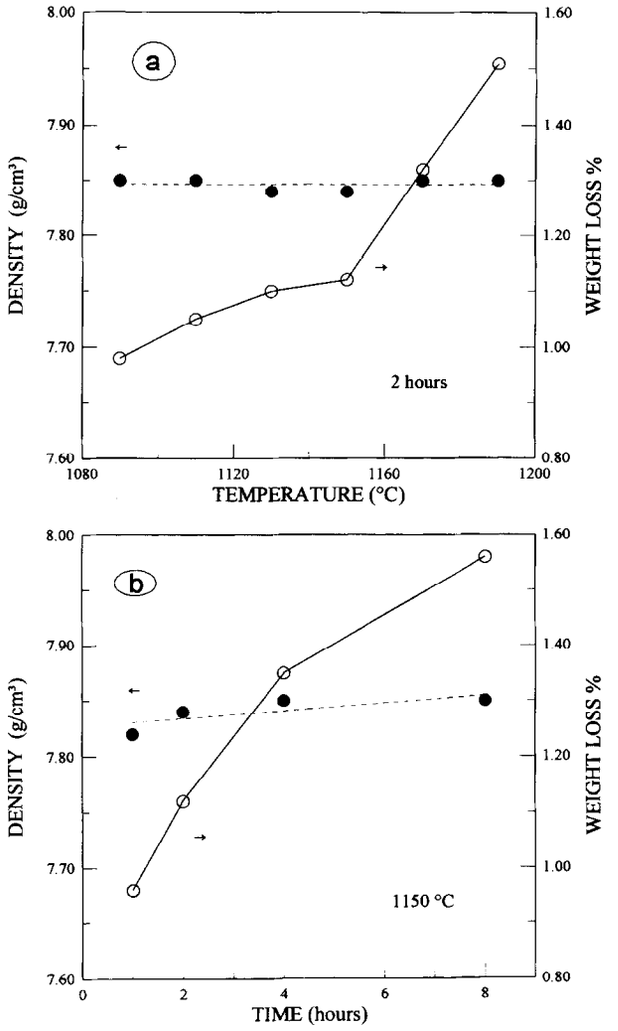

Fig. 1. Apparent density and weight loss of PZT iron-doped ceramics sintered at different (a) temperatures and (b) times.

The average grain size of 1·20 μm (Fig. 2) showed small variations with sintering treatment having a similar behaviour than the apparent density of the ceramics. A grain size increase of 40% in respect to the starting particle size approximately could be observed.

The microstructure of these ceramics was very homogeneous and the mayor difference between them was observed by SEM on fresh fractured surfaces (Fig. 3). When the weight loss increased a change on the fracture behaviour from intragranular to intergranular fracture type occurs.

The microstructure observed by TEM revealed the existence of non-ferroelectric phases. Figure 4(a) shows the microstructure of sample sintered at 1090°C for 2 h. Up to 30 nm PbO-rich pockets [P in Fig. 4(a)] at the triple junctions of three grains were detected as corresponding with the EDS spectra collected. The difference in the PbO amount between the grains and the triple junction phase was obvious. Both phases showed traces of silica as impurity. The microstructure of the sample 1150°C/2 h differed substantially from the microstructure of other sintered samples (Fig. 5). The sample was polyphase, besides PZT grains, ZrO_2 monoclinic grains and PbO-rich phase at the pockets between grains were founded. Two types of ZrO_2 were observed [Fig. 5(a)]: larger grains (up to 0·5 μm) with a characteristic twin structure and small (less than 100 nm) precipitates which were untwinned. The twinned ZrO_2 grains were surrounded by PZT grains and PbO-rich phases, meanwhile the small untwinned ZrO_2 precipitates were spherical shaped and were located inside PZT grains. EDS analysis of PbO-rich phase [Fig. 5(d)] showed high silica content but no relevant Ti^{4+} cations presence. Figure 6 shows the TEM micrograph and EDS spectra of 1180°C/2 h sintered sample. Only secondary PbO-rich phase at triple point junctions having Ti^{4+} and Zr^{4+} cations in their composition were detected at this temperature. From the TEM observations it was difficult to conclude if the liquid was located at the grain boundaries or if it is only located at the pockets.

3.2 Dielectric and piezoelectric properties

Dielectric constant and dielectric losses of the ceramics sintered at different temperatures and

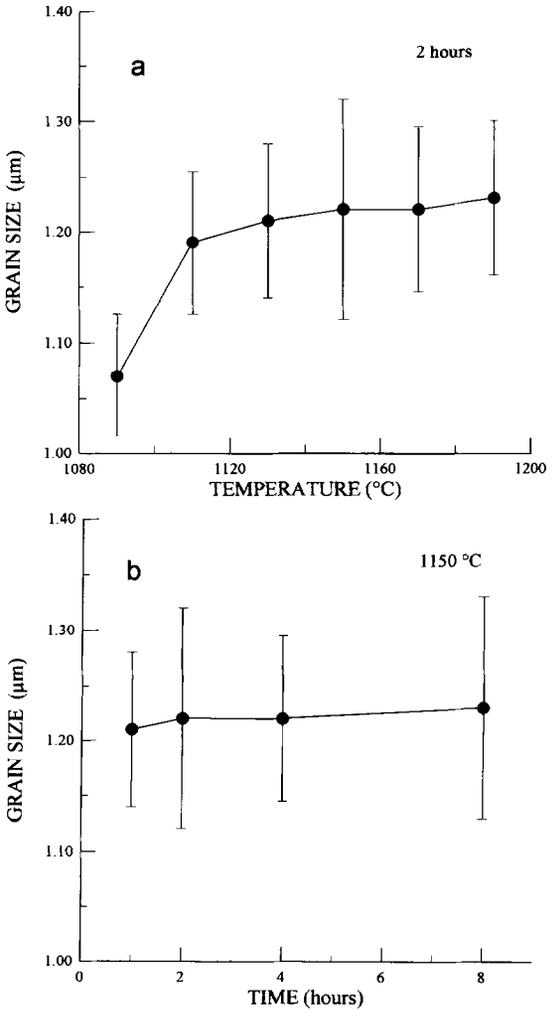

Fig. 2. Grain size of PZT iron-doped ceramics sintered at different (a) temperatures and (b) times.

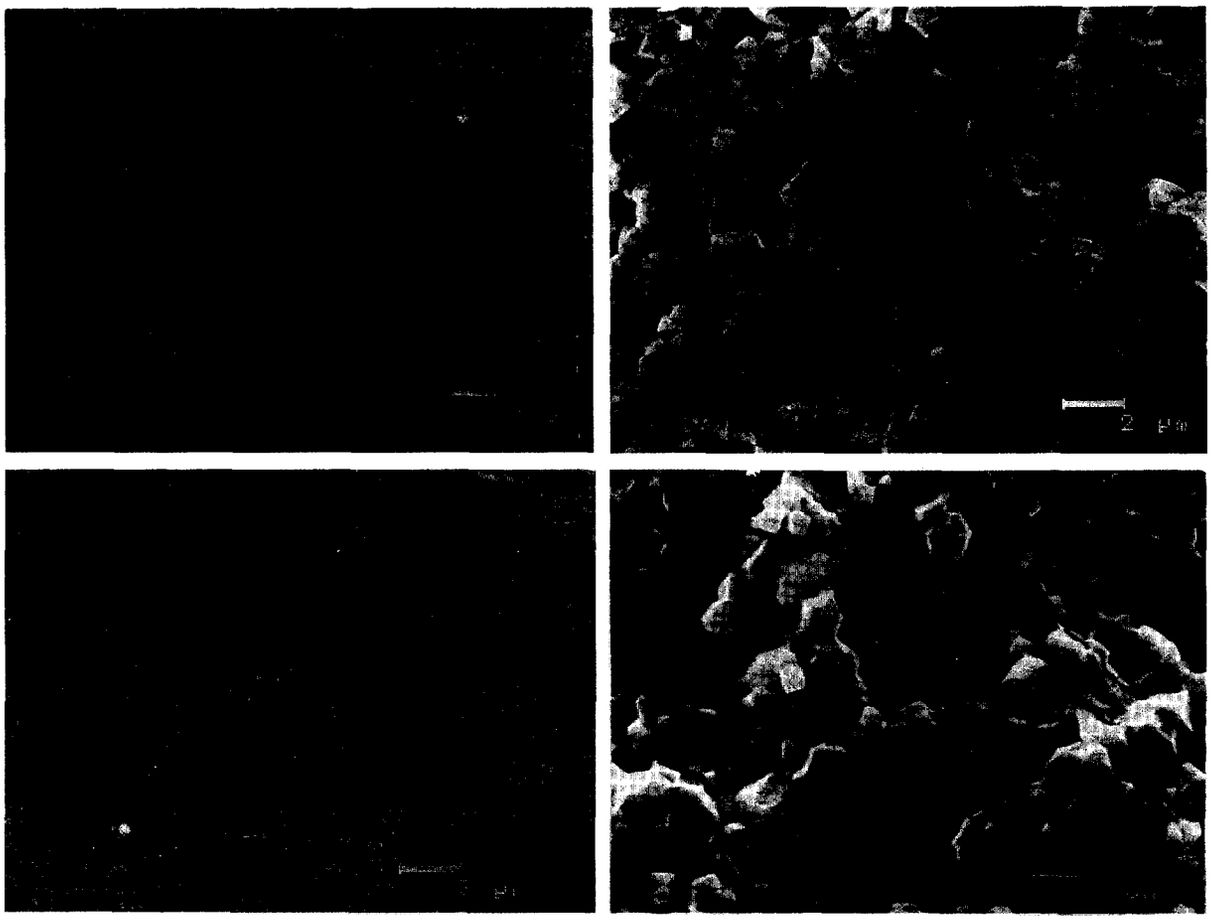

Fig. 3. SEM micrographs of PZT iron-doped ceramic sintered at 1150°C. Polished and chemical etched surfaces, and fresh fracture surface of (a,b) 2 h and (c,d) 8 h, respectively.

times showed a maximum and a minimum respectively (Fig. 7). The maximum dielectric constant and the minimum dielectric losses took place for the samples sintered at the temperature and time which presented the inflection point in weight loss, 1150°C/2 h. Higher sintering temperatures and times kept with an sluggish reduction the value of dielectric constant and increased the dielectric losses.

The electromechanical coupling factors in the planar and thickness modes of poled fine grained PZTs were unconnected with the grain size (Fig. 8). The planar mode coupling factor was lower than the thickness mode one for low sintering temperatures and times, but reached the higher value for 1150°C/2 h sintered ceramic. On the other hand, the mechanical quality factor reached a maximum for this sintered sample.

3.3 Decomposition experiments

The sample sintered for 2 h was less sensitive to the decomposition effect than the 8 h one (Fig. 9). The 2 h sintered sample needed $\approx$120 min to decompose in a mixture of tetragonal phases with different c/a ratio meanwhile the 8 h sintered sample only needed 5 min to reach the same decomposition level. The 2 h sintered sample had a surface with a rhombohedral/tetragonal ratio r/t = 1·64, higher than the measured for the 8 h sample r/t = 1·09.

XRD of the decomposed surface (Fig. 10) always presented monoclinic zirconia traces and PbO as secondary crystalline phases.

The decomposition occurred with weight loss in the range of 1 wt%. Taking into account that the weight loss took place preferentially at the surface of the sintered sample there was a considerable removal of mass at that region, mainly lead cations, but not quantification of the vaporisation process was attempted. The microstructure of 2 h sample decomposed during 120 min showed (Fig. 11) a roughness surface that indicated preferential mass removal. The grains did not well defined in the microstructure. The valley areas of the decomposed surfaces were plenty of big grains [Fig. 11(b)]. The microstructure of 8 h sample decomposed during 5 min was quite different that the 2 h one (Fig. 12). Even if the same level of decomposition was reached (XRD patterns and weight loss), the surface had a less cohesive microstructure with big faceted grains. There was a rim area near the border of the disk in which rest of liquid phase still appeared.

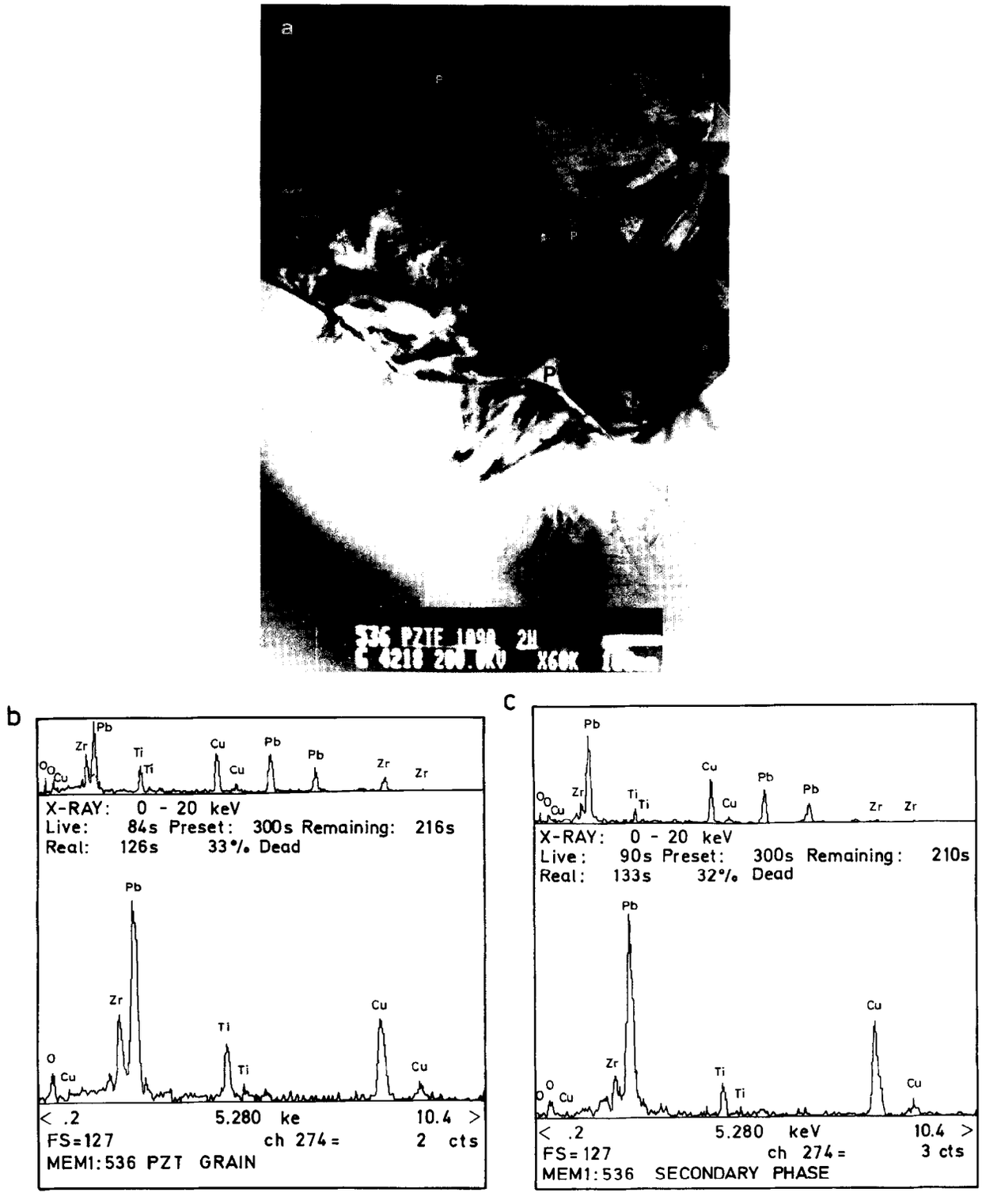

Fig. 4. TEM micrograph of the sample sintered at (a) 1090°C 2 h, with the EDS spectra of (b) the grain and (c) the secondary phase quoted at P in the micrograph.

4 Discussion

The used milling procedure was shown to be very effective in the production of submicronic PZT powders. The small particle size allowed the compacts to sinter at lower temperatures than commercial PZT. The differences in dielectric and piezoelectric properties of samples sintered at different temperatures were relevant and independent of grain size. On the other hand, there were two phenomena that are necessary to correlate: weight loss became more relevant for temperatures higher than 1150°C and increased with time; the microstructural differences were related to the nature and evolution of the second phases.

The presence of a liquid in the early stage of sintering could be related to unreacted or free PbO. If the iron cations did not reached the solid

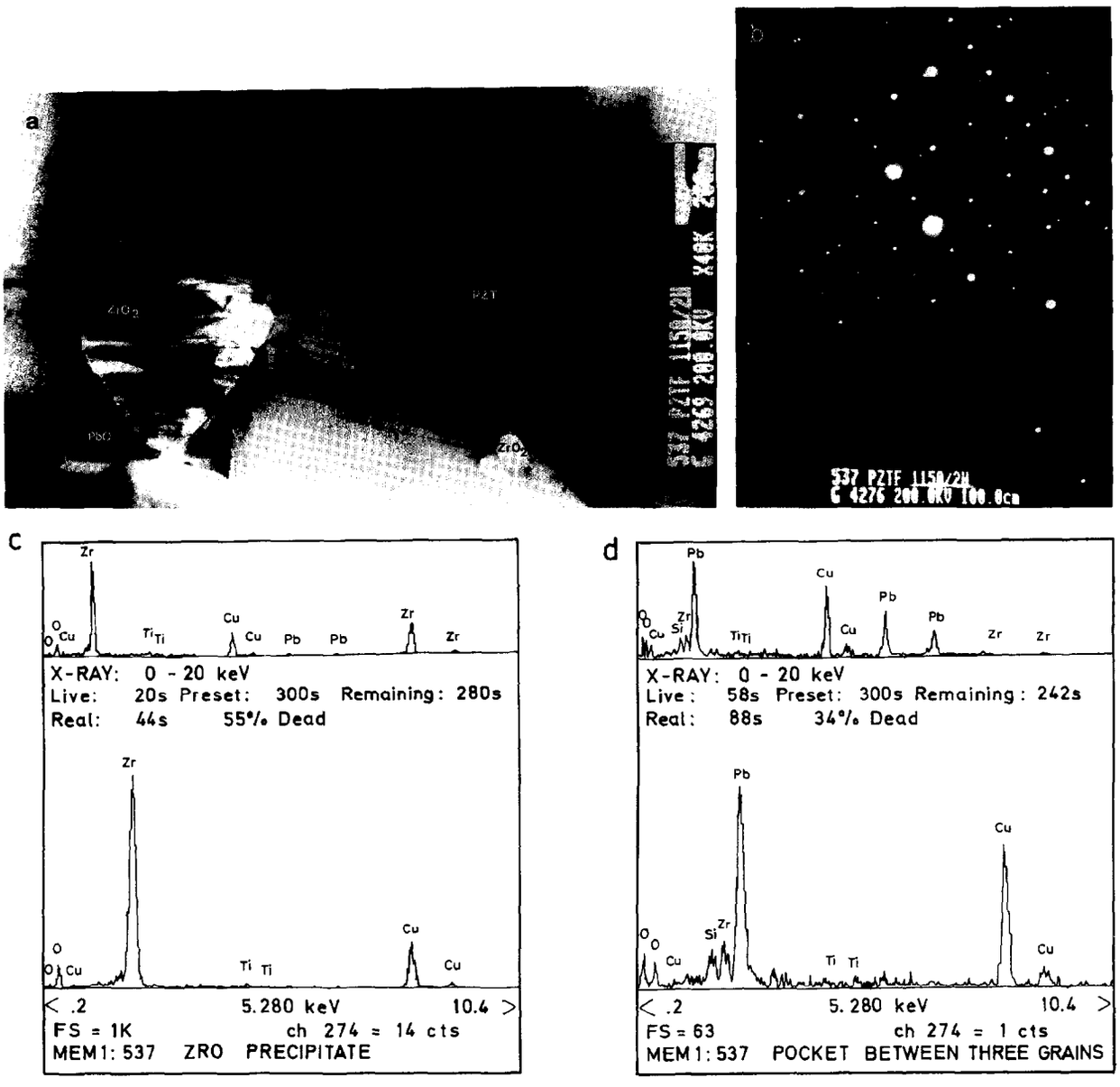

Fig. 5. (a) TEM micrograph of the sample 1150°C 2 h. (b) The selected area electron diffraction pattern of twinned ZrO_2 grain. EDS spectra of (c) the twinned ZrO_2 grain and (d) the secondary phase quoted at PbO in the micrograph.

solution at this sintering stage, as the piezoelectric properties revealed, the amount of PbO that has been dosified to preserve the stoichiometry could remain as unreacted material. Thus, the excess of PbO could be located in the neck areas as consequence of the capillary forces and the buffered atmosphere prevented the removal of lead cations. The lead content in the PbO-rich liquid could increased by adsorption of atmospheric lead cations from the buffered atmosphere but there was no evidence of weight gain. The buffer assumed the function to keep the PbO vapour pressure constant. Higher levels of weight loss were detected for the buffer when sintering was performed at temperatures $\geq$1150°C. All the samples had the same densification level, and in a first approach there was no correlation between densification level and weight loss. The weight loss need to be independent of dopant, but if the homogeneity is incomplete, the changes in dopant distribution could be translated to variations in weight loss. Weston *et al.*[13] established that Fe^{3+} enters the B sites in lead zirconate-lead titanate, and substitutes Ti^{4+} or Zr^{4+} ions. Sintering lead zirconate-lead titanate iron-doped samples without excess of PbO led to weight gains of 2 mole of PbO for each mole of Fe_2O_3 added. In the present case, the weight loss could be in contradiction with the established weight gain, but it is necessary to point out that the iron addition was compensated in the starting composition with the corresponding amount of PbO in order to obtain stoichiometric PZT ceramics. So, when iron cations entered into the lattice in B positions, an equal number of Pb atoms filled the newly created A sites.[13] The weight loss detected could be attributed in part to water,

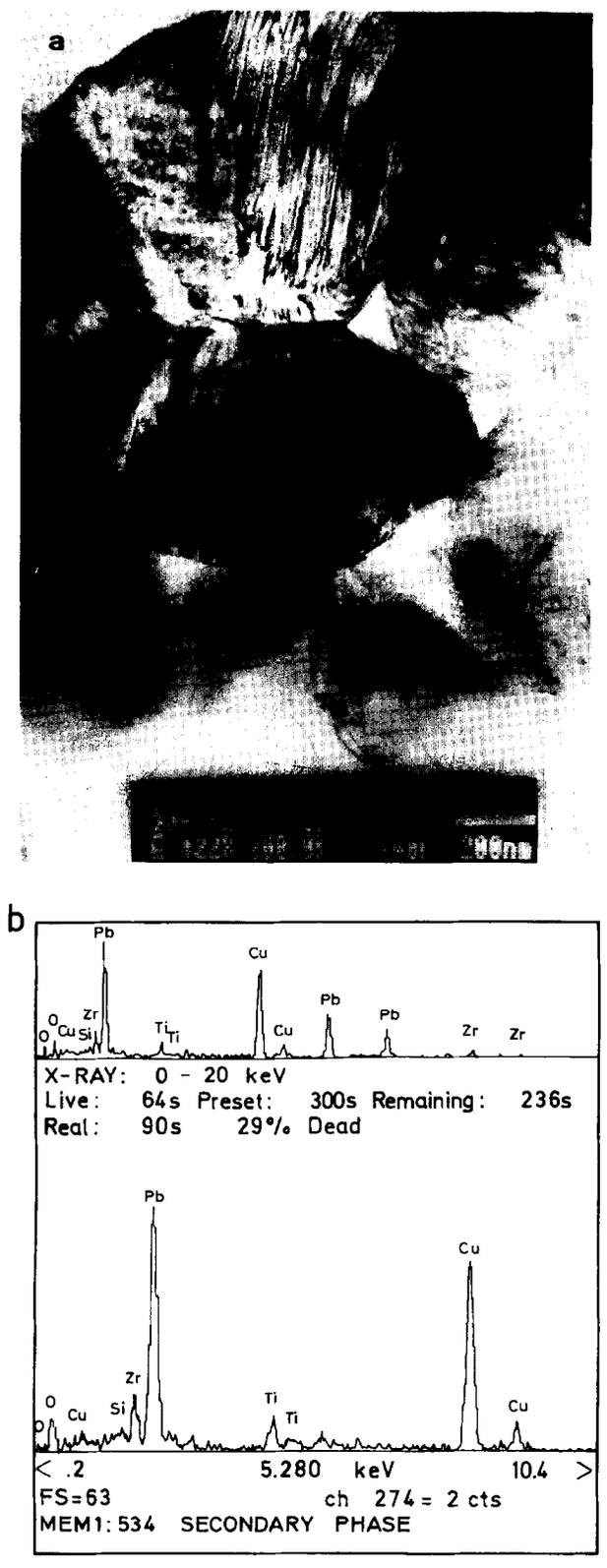

Fig. 6. (a) TEM micrograph of the sample sintered at 1180°C 2 h with (b) the EDS spectra of the secondary phase.

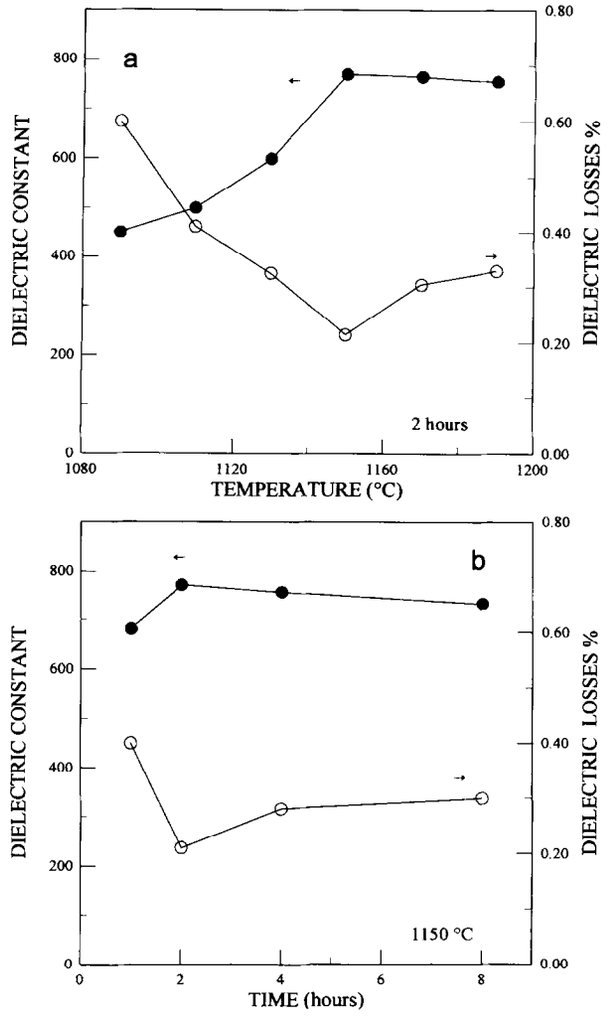

Fig. 7. Dielectric constant and dielectric losses of PZT iron doped ceramics sintered at different (a) temperatures and (b) times.

alcohol and organic contamination of the surface of the powders that were eliminated at lower temperatures than the sintering one, or in part with the charge compensation created by Nb^{5+} that produces lead vacancies.[14] But, even if it is assumed that the weight loss detected for the samples sintered well below 1150°C were all of them attributed to such powder contamination, the weight loss for temperatures higher than 1150°C must be clearly related to the evolution of PbO-rich phase present in all the samples.

Although the grain-boundary phase was PbO-rich, it remained amorphous when solidified. The amorphous nature of the grain boundary phase may be due to the geometry or microstructure rather than the composition.[15] The presence of silica as an impurity favoured the tendency to form glass. The presence of secondary PbO-rich phase was notorious but both the small grain size and the high densification level over a wide range of temperatures and times were not modified. The PbO-rich phase observed in the pocket regions at temperatures lower than 1150°C contains Ti^{4+} and Zr^{4+} cations. The formation of a liquid which has a high solubility for PZT is consistent with the $PbO–PbTiO_3–PbZrO_3$ phase diagram.[16] However, the composition of such a liquid is expected to be close to the $PbO–TiO_2$ eutectic which occurs at approximately 89 mole% PbO at 838°C.[16] In the

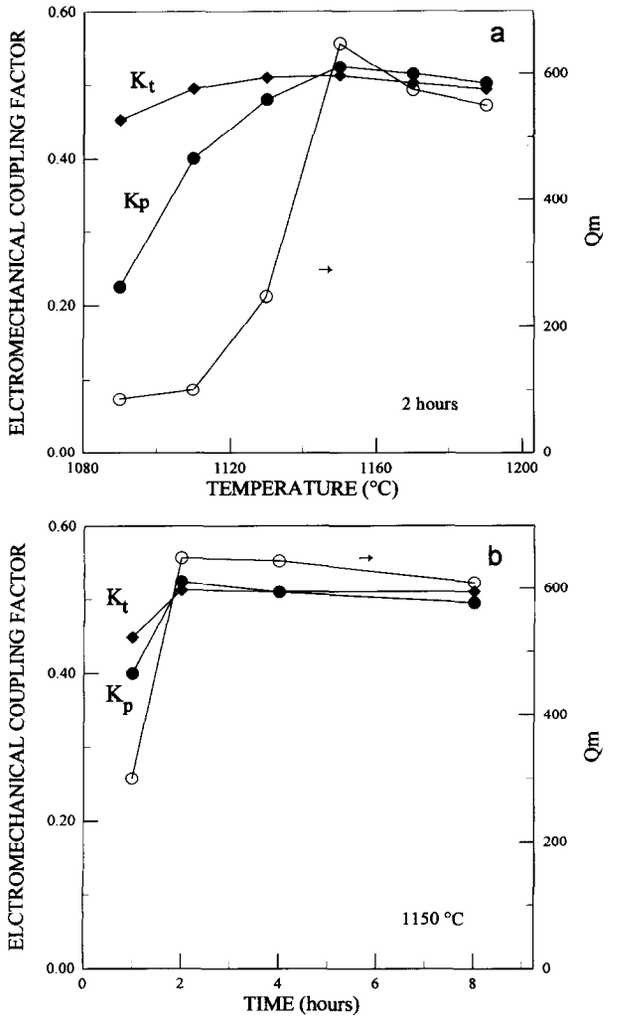

Fig. 8. Electromechanical coupling factors and mechanical quality factors of PZT iron doped ceramics sintered at different (a) temperatures and (b) times.

early stage of sintering transport of PbO to particle surfaces and grain boundaries occurs via a vaporisation/condensation mechanisms due to the high PbO partial pressure.[17] The presence of Ti^{4+} and Zr^{4+} in the liquid suggests that it dissolved solid PZT. Such a liquid only promoted slight coarsening during the early stage of sintering. The grains grew up to 1·20 μm from the starting particle size of 0·85 μm, and there was no grain growth during the final stage of sintering.

The dopant effects were relevant if dielectric properties are taken into account. The dielectric constant reached a maximum value and the dielectric losses a minimum for samples sintered at 1150°C/2 h. The maximum value of the dielectric constant, ~780, was slightly higher than the dielectric constant reported by Weston *et al.*[13] for a dopant level of ~0·5 mol% $FeO_{1.5}$ per mol of PZT (0·8 wt% of Fe_2O_3). In the present work the iron cations were partially compensated with the presence of niobium cations. However, if the mechanism for reaching the reported value of dielectric constant is the incorporation of iron cations onto B positions of the perosvkite lattice, then iron amounts lower than 0·5 mol% $FeO_{1.5}$ per mol of PZT must given higher dielectric constant, this fact is clearly in contradiction with the measured values of high densified low sintering temperatures samples. So, it seems that iron cations enter into the PZT crystalline lattice for a sintering treatment of 1150°C/2 h or at higher temperatures and longer times.

For the samples sintered at 1150°C/2 h there was a PbO-rich phase at the grain boundaries and it composition is located in the zirconium rich region, with the presence of discrete ZrO_2 monoclinic

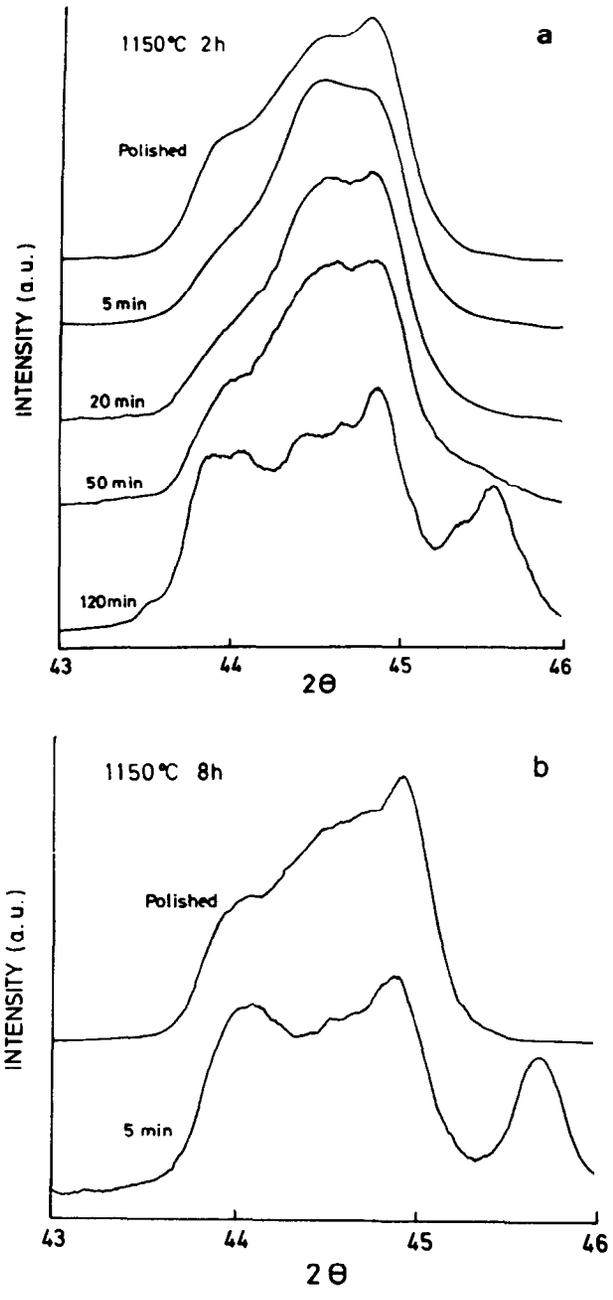

Fig. 9. DRX pattern for different decomposition times of thermal treated polished surfaces of samples sintered at 1150°C for (a) 2 h and (b) 8 h.

grains. The dielectric properties made evidence this change in composition. The piezoelectric parameters showed that during such a compositional change, the iron cations enter into the perovskite structure because the electromechanical parameters reached values expected for such a doping level, if considering the presence of Nb^{5+} cations.[18] Higher sintering temperatures and times produced newly the appearance of a secondary PbO-rich phase having Ti^{4+} and Zr^{4+} cations on its composition. The grain size remained quite similar for most of the ceramics under study, but the incorporation of Fe^{3+} into the crystalline lattice seemed to affect more markedly the dielectric properties and the Q_m. The coupling factors were relatively independent of the dopant content.

The first PbO-rich liquid was formed in the system PbO–PZT. The doping ions seemed to be concentrated near the grain boundaries and substantially reduced their mobility. When the boundary moved, it must adsorbed the excess dopant with it.[19] As a consequence of the Fe^{3+} incorporation into the PZT the charge compensation mechanism produced oxygen vacancies that

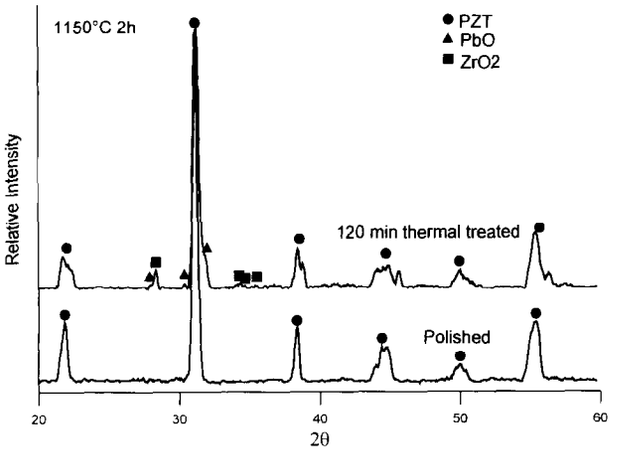

Fig. 10. DRX patterns of 1150°C 2 h sintered samples. Surface as polished and thermally treated for 120 min.

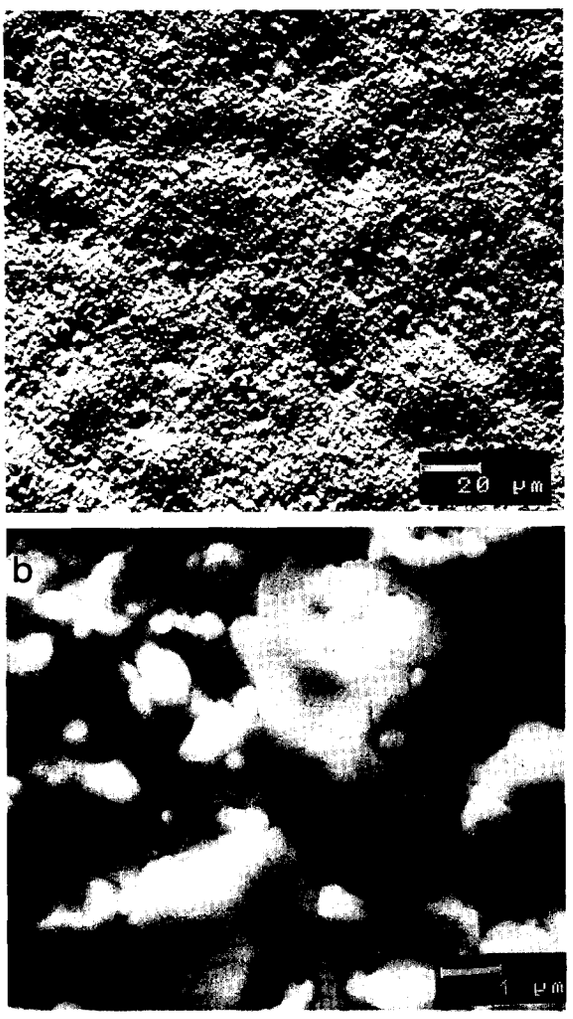

Fig. 11. SEM micrograph of decomposed surface after 120 min thermal treatment of 1150°C/2 h (a) sintered sample and (b) high magnification of a valley area.

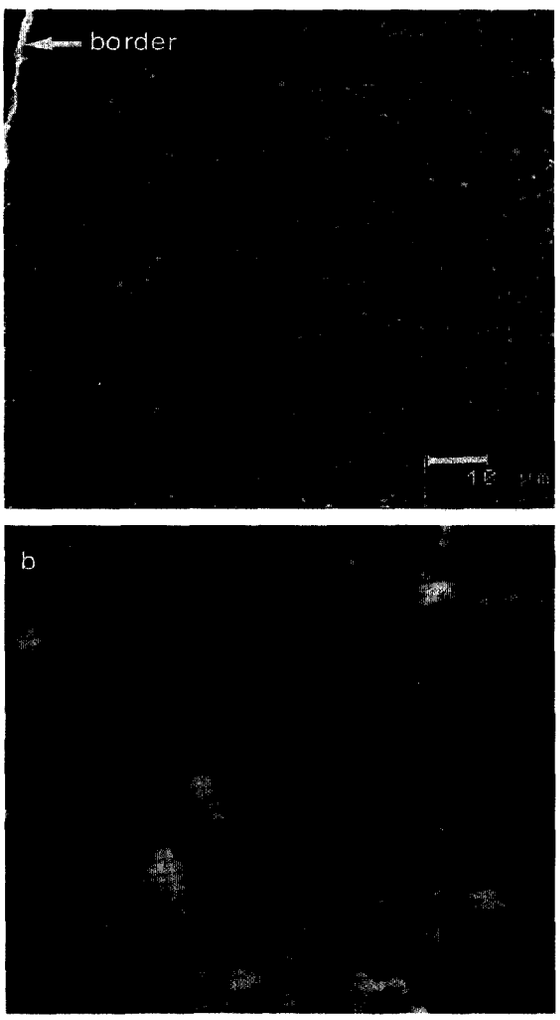

Fig. 12. SEM micrograph of decomposed surface after 5 min thermal treatment of 1150°C/8 h sintered sample showing (a) the border effect and (b) high magnification of centre of the sample.

Fig. 13. TEM micrograph of 1150°C/2 h sintered sample shown antiphase boundaries (APB) of ferroelectric tetragonal symmetry.

are the slowest-moving species, and hence, rate-limiting.[19] When the dopant entered the PZT lattice the secondary phase had a composition in the PbO–PZ system. In this system, there is a peritectic point and the PbO could dissolve up to 4 mole% of ZrO_2.[16] Thus a Zr-rich lead zirconate titanate regions seemed easier to be dissolved than Ti-rich ones. The mechanism proposed by Saha and Agrawal[16] could be the responsible for the appearance of ZrO_2 monoclinic grains beside PZT ones. Small ZrO_2 spherical shaped precipitated inside the PZT grains are assumed to be unreacted particles,[15] because they also appeared in samples sintered at other temperatures. The difference founded with the proposed mechanism was related to the fact that PbO was not completely eliminated because the porosity was closed at that densification level. This mechanism was supported by the existence of grains with tetragonal domain patterns and antiphase boundaries (Fig. 13). However it was not clear how the dopant incorporation can reduce the presence of Ti^{4+} cations in the remained liquid. Recently, it was reported in La-doped PZT, the existence of and enrichment of Zr^{4+} at the grain boundaries regions among with a PbO-rich phase in the triple point junction as well in grain boundary films.[20] Once the dopant has been incorporated into the lattice and at higher sintering temperatures the liquid recovered a composition with Zr^{4+} and Ti^{4+} cations.

The observed crystalline phase evolution of the thermally decomposed samples is in concordance with the proposed decomposition mechanism[6] which moved to the tetragonal symmetry as lead oxide was removed from the lattice. Low decomposition times displaced slightly the phase content toward the rhombohedral region, effect that could be related to the higher incorporation of iron cations to the lattice and the corresponding change of the MPB to lead Zr-rich part of the phase diagram for Fe-doped PZT ceramics.[13]

The 2 h sintered sample has liquid with a composition in the PbO–PZ system. When heating without PbO buffering, such a secondary phase melted and dissolved PZT grains before the eutectic composition was reached. The elimination of PbO by evaporation left some Ti-rich PZT grains and ZrO_2 according with eqn (1). One open question is if the dissolution of PZT grains proceeds preferentially based on compositional fluctuations. In the 8 h sintered sample, the liquid composition is eutectic an the PbO evaporation occurs suddenly and the decomposition reaction progressed.

5 Conclusions

PZT acceptor-doped fine-grained piezoelectric ceramics were processed from solid state reaction at higher temperature. The double milling process had shown to be very effective in the production of submicronic PZT synthesised powders. The differences in the dielectric and piezoelectric properties of samples sintered at different temperatures and times were relevant and quite independent of grain size. The dopant incorporation to the PZT solid solution was the responsible phenomenon of the nature and evolution of the secondary phases and weight loss. The properties were related to the incorporation of the iron cations into the PZT crystalline lattice.

At the initial stage of sintering there was a PbO-rich intergranular phase. When the acceptor cation entered into the crystalline lattice the oxygen vacancies appeared and the densification process was governed by a drag mechanism that effectively inhibited grain growth. The initial PbO-rich liquid dissolved PZT grains and enriched the liquid in Zr^{4+} and Ti^{4+} cations. When iron cations entered into the solid solution, the secondary phase displaced to a liquid in the PbO–PZ system with appearance of both the ZrO_2 monoclinic precipitates and the tetragonal PZT grains due to the limited solubility of Zr^{4+} in this system. Higher temperatures and times produced new enrichment

of Ti^{4+} and Zr^{4+} cations of the PbO-rich liquid by dissolution of PZT grains with an increasing of weight loss due to lead oxide removal.

The nature of the liquid was revealed by thermal decomposition studies on polished surfaces. The decomposition progressed quickly in samples having liquid in the PbO–PZT system.

Acknowledgements

The authors express their gratitude to the following agencies for financial support of this work: European Commission (COST 503), Spanish Science Ministry (CICYT MAT 94-807 and MAT 97-0694-CO2-01) and Slovenian Ministry for Science and Technology.

References

1. Jaffe, B., Cook Jr, W. R. and Jaffe, H., *Piezoelectric Ceramics*. Academic Press, London, 1971.
2. Ari-Gur, P. and Benguigui, L., X-ray study of the PZT solid solution near the morphotropic phase transition. *Solid State Com*, 1974, **15**, 1077–1079.
3. Mabud, S. A., The morphotropic phase boundary in PZT solid solutions. *J. Appl. Cryst*, 1980, **13**, 211–216.
4. Kakegawa, K. and Mohri, J., A Compositional fluctuation and properties of $Pb(Zr,Ti)O_3$. *Solid State Com*, 1977, **24**, 769–772.
5. Kakegawa, K., Mohri, J., Shiraseki, S. and Takahashi, K., Sluggish transition between tetragonal and rhombohedral $Pb(Zr,Ti)O_3$ prepared by application of electric field. *J. Am. Ceram. Soc.*, 1982, **65**(10), 515–519.
6. Saha, S. K. and and Agrawal, D. C., Compositional fluctuations and their influence on the properties of lead zirconate titanate ceramics. *Am. Ceram. Soc. Bull.*, 1992, **71**(9), 1424–1428.
7. Lloyd, I. K., Kahn, M. and Lang, S., Effect of microstructural heterogeneities on piezoelectric behaviour of PZT ceramics. In *Ceramic Transaction Vol. 8, Dielectric Ceramic: Composition, Processing and Properties*, ed. H. C. Ling and M. Yan. The American Ceramic Society, Westerville, OH, 1990, pp. 390–398.
8. Fernandez, J. F., Nieto, E., Moure, C., Duran, P. and Newnham, R. E., Processing and microstructure development of porous and dense PZT thick films on Al_2O_3. *J. Mater. Sc.*, 1995, **30**, 5399–5404.
9. Moure, C., Villegas, M., Fernandez, J. F. and Duran, P., Microstructure and piezoelectric properties of fine grained PZT ceramic doped with donor and/or acceptor cations. *Ferroelectrics*, 1992, **127**, 113–118.
10. Snow, G. S., Elimination of porosity in $Pb(Zr,Ti)O_3$ ceramics by liquid phase sintering. *J. Am. Ceram. Soc*, 1974, **57**(6), 272.
11. Cheng, S., Lloyd, I. K. and Khan, M., Modification of surface texture by grinding and polishing lead zirconate titanate ceramics. *J. Am. Ceram. Soc*, 1992, **75**(8), 2293–2296.
12. IRE standart on piezoelectric crystals: determination of elastic, piezoelectric and dielectric constant—the electromechanical coupling factor. *Proc IRE*, **46**, 1958, 764–778.
13. Weston, T. B., Webster, A. H. and MacNamara, V. M., Lead zirconate-lead titanate piezoelectric ceramics with iron oxide additions. *J. Am. Ceram. Soc*, 1969, **52**(5), 253–257.
14. Atkin, R. B., Holman, R. L. and Fulrath, R. M., Substitution of Bi and Nb ions in lead zirconate-titanate. *J. Am. Ceram. Soc*, 1971, **52**(2), 113–115.
15. Goo, E. K. W., Mishra, R. K. and Thomas, G., Transmission electron microscopy of $Pb(Zr_{0.52}Ti_{0.48})O_3$. *J. Am. Ceram. Soc.*, 1981, **64**(9), 517–519.
16. Fushimi, S. and Ikeda, T., Phase equilibrium in the system $PbO–PbTiO_3–PbZrO_3$. *J. Am. Ceram. Soc.*, 1967, **50**(3), 129–132.
17. Akbas, M., McCoy, M. A. and Lee, W. E., Microstructural evolution during pressureless sintering of lead lanthanum zirconate titanate ceramics with excess lead(II) oxide. *J. Am. Ceram. Soc*, 1995, **78**(9), 2417–2424.
18. Takahashi, S., Effects of impurity doping in lead zirconate titanate ceramics. *Ferroelectrics*, 1982, **41**, 143–156.
19. Atkin, R. B. and Fulrath, R. M., Point defects and sintering of lead zirconate-titanate. *J. Am. Ceram. Soc.*, 1971, **54**(5), 265–7020.
20. Hammer, M., Hoffmann, M. J. and Baretzky, B., Characterisation of chemical inhomogeneities in doped and undoped PZT ceramics. In *Electroceramics V* Vol 1, ed. J. L. Baptista, J. A. Labrincha and P. M. Vilarinho. Tipave, Aveiro, Portugal, 1996, pp. 161–164.